Stratospheric ozone intrusions and impacts on tropospheric ozone

Jesse Greenslade[1], Simon Alexander[2], Robyn Schofield[3,4], Jenny A. Fisher[1,5], and Andrew Klekociuk[2]

[1]*Center for Atmospheric Chemistry, School of Chemistry, University of Wollongong*
[2]*Australian Antarctic Division, Hobart*
[3]*School of Earth Sciences, University of Melbourne*
[4]*ARC Centre of Excellence for Climate System Science, University of New South Wales*
[5]*School of Earth & Environmental Sciences, University of Wollongong*

September 17, 2016

Abstract

We develop a quantitative method to identify Stratosphere to Troposphere Transport events (STTs) from ozonesonde profiles. Using this method we estimate the quantity of ozone transported across the tropopause over Melbourne (38°S), Macquarie Island (54°S), and Davis (69°S). STT seasonality is determined from a 7–9 year long time series of ozone profiles from each site. STT events primarily occur during summer above Melbourne and Macquarie Island, while there is little seasonal cycle in STT events above Davis. The majority of tropospheric ozone due to STT events occur within 3 km below the tropopause at Melbourne and Macquarie Island, and within 2 km below the tropopause at Davis. Overall, the fraction of total tropospheric ozone attributed to STT events is 2 – 4% at each site, however, during individual events, an STT event can contribute more than 10% of the total tropospheric ozone at that time. We use the GEOS-Chem model to understand out point-source ozonesonde results in a 3-dimensional context. The GEOS-Chem model run with active stratospheric chemistry is too coarsely resolved in the vertical dimension to determine STTs. Simulated seasonal cycles of tropospheric ozone are well matched at all three sites although vertical profile averages have some bias in the troposphere compared with ozonesondes. A conservative estimate of yearly tropospheric ozone flux due to STTs is calculated using the simulated tropospheric ozone column between 35°S and 75°S of 2.2×10^{16} molecules cm^{-2} yr^{-1} (TODO: update number once model finishes).

1 Introduction

Tropospheric ozone constitutes only 10% of the total ozone column but is an important oxidant and greenhouse gas and is toxic to life, harming natural ecosystems and reducing agricultural productivity.. Over the industrial period, increasing tropospheric ozone has been estimated to exert a radiative forcing equivalent to a quarter of the CO_2 forcing [Forster et al., 2007]. Further tropospheric ozone enhancements above pre-industrial levels are projected to drive reductions in global crop yields equivaltent to losses of up to $\$USD_{2000}$ 35 billion per year (simulated until 2030) [Avnery et al., 2013] along with detrimental health outcomes equivalent to ∼11.8 billion per year by 2050 [Selin et al., 2009]. Tropospheric ozone is produced photochemically NO_x and volatile organic compound emissions, which have both anthropogenic (fossil fuel, biomass combustion) and natural (wildfires, lightning, biogenic) sources. In the upper troposphere, downward transport from the ozone-rich stratosphere provides an additional natural source of tropospheric ozone(Jacobson and Hansson [2000] and references therein).

Stratosphere-to-troposphere transport (STT) primarily impacts the ozone budget in the upper troposphere but can also increase regional surface ozone levels above the legal thresholds set by air quality standards [Danielsen, 1968, Lefohn et al., 2011, Langford et al., 2012, Zhang et al., 2014]. A review of two photochemical models by Stohl et al. [2003] concluded that between 25-50% of tropospheric ozone column can be attributed to SST events, although this mostly affects the upper troposphere. A lower estimate was derived from the Atmospheric Chemistry and Climate Model Intercomparison Project (ACCMIP), Stevenson et al. [2006] found STT was responsible for only ∼ 10% (equivalent to 550 ± 170 Tg/yr), with the remainder produced photochemically. The wide range in model estimates exists in part because models are challenged to correctly represent STT. Observation-based process studies are therefore key in determining the relative frequency of SST to the troposphere, with models then able to use this to quantify STT impact over large regions.

STT events are due to deep overshooting convection [Frey et al., 2015], tropical cyclones [Das et al., 2016] and mid-latitude synoptic scale disturbances (e.g. Stohl et al. [2003], Mihalikova et al. [2012]). STT events are strongly dependent on both season and location, for instance over the Mediterranian region, a 10% contribution to tropospheric ozone is estimated between 2000 and 2003 [Galani, 2003], with Lefohn et al. [2011] noting strong seasonal dependance. Notably, STTs have been shown to contribute up to 30% of the surface ozone over the Western US in spring [Lin et al., 2012].

To date, while the frequency, seasonality, and impacts of STT events have been well characterised in the tropics and Northern Hemisphere (NH), observational estimates from the Southern Hemisphe (SH) extra-tropics are noticeably absent from the literature. Since 1998 NASA has tried to standardise ozonesonde release procedures and improve measurement frequency in the SH through the Southern Hemisphere ADditional OZonesonde (SHADOZ) website (`http://croc.gsfc.nasa.gov/shadoz/`). The papers which have focused on

tropospheric ozone in the SH also note the difficulties that arise from sparse datasets, as many of the sonde releases only occur every two to four weeks and far fewer release sites exist compared to the NH [Liu et al., 2015, Thompson et al., 2014, Mze et al., 2010]. This is further complicated due to ozone intrusion events sometimes lasting for just a matter of hours [Tang and Prather, 2012]. Recently ozonesondes were analysed showing upper tropospheric ozone is increasing near southern Africa, with the increase most likely due to stratospheric mixing [Liu et al., 2015, Thompson et al., 2014]. The extra-tropics in the SH have even less observational studies published.

In the extra-tropics, ozone has a longer photochemical lifetime(TODO: how long?) and STT events most commonly occur during synoptic-scale tropopause folds [Sprenger et al., 2003, Tang and Prather, 2012], and are characterised by tongues of high potential vorticity (PV) air descending to low altitudes. As these tongues become elongated, filaments disperse away from the tongue and mix irreversibly into the troposphere. To date, STT events have been observed in tropopause folds around both the polar front jet [Vaughan et al., 1993, Beekmann et al., 1997], and the subtropical jet [Baray et al., 2000]. They are also observed near cut-off lows [Price and Vaughan, 1993, Wirth, 1995], some of the stratospheric mixing may be due to the turbulent weather which often accompanies these cut-offs. A high correlation has been found between lower stratospheric and tropospheric ozone concentrations [Terao et al., 2008], suggesting mixing between these two layers, with jet streams over the ocean being the major source of transport between the layers.

Here, we use nearly a decade of ozonesonde observations from three locations spanning latitudes from 38°S - 69°S to characterise the seasonal cycle of STT events and quantify their contribution to the tropospheric ozone budget. In Section 2 we describe the observations and the methods used to identify STT. In Section 3 we examine two case studies to relate STT occurrence to meteorological events. Section 4 provides our newly derived climatologies of STT frequency, seasonality, intrusion altitude, and depth. Section 5 uses these new climatologies to evaluate tropospheric ozone in a global chemical transport model (GEOS-Chem). Finally, we use the observations and the model to estimate the overall contribution of STT events to total tropospheric ozone in the high southern latitudes.

2 Data and Methods

2.1 Ozonesonde record in the Southern Ocean

Ozonesondes provide a high vertical resolution profile of ozone, temperature, pressure, and humidity from the surface to 35 km.

Ozone mixing ratio is quantified with an electrochemical concentration cell that senses the proportional electrical current from reaction of ozone with a solution of potassium iodide. Standardised procedures are followed when constructing, transporting, and releasing the ozonesondes [NOAA]. Ozonesondes

are estimated to provide around 2% precision in the stratosphere, which improves at lower altitudes [NOAA], although the ozonesondes have been shown to be accurate to within 5% as long as the correct procedures are followed [Smit et al., 2007].

Ozonesondes are launched approximately weekly from Melbourne (38°S, 145°E), Macquarie Island (55°S, 159°E) and Davis (69°S, 78°E). For this study, we use the data collected from 2004-2013 for Melbourne and Macquarie, and 2006-2013 for Davis. This is because at these dates we have both ozone and geopotential height (GPH) profiles from the ozonesondes at these sites. At Davis, ozonesondes are launched twice as frequently in the months just prior to and during the ozone hole season (June-October) as at other times of the year [Alexander et al., 2013].

Stratospheric ozone typically mixes irreversibly (vertically and horizontally) into the troposphere in kilometre-scale tongues of air [Frey et al., 2015]. The strength (ozone enhancement above background levels), horizontal scale, vertical depth, and longevity of these intruding ozone tongues vary with weather, topography, and season. This makes the vertical ozone profile recorded by the ozonesonde highly dependent on the time of launch [Sprenger et al., 2003], and it cannot be guaranteed that detected ozone enhancements are fully separated from the stratosphere.

haracterisation of STT events requires a clear definition of the tropopause. The two most common tropopause height definitions are the standard lapse rate tropopause [WMO, 1957] and the ozone tropopause [Bethan et al., 1996]. The lapse rate tropopause is defined as the lowest altitude where the lapse rate (gradient of temperature with altitude) is less than 2° C km^{-1}, provided the lapse rate between this altitude and all subsequent altitudes within 2 km is also below 2° C km^{-1}. The ozone tropopause is defined as the lowest altitude satisfying the following three conditions for the ozone mixing ratio (OMR) [Bethan et al., 1996]:

1. Vertical gradient of OMR is greater than 60 ppbv km^{-1}
2. OMR is greater than 80 ppbv
3. OMR exceeds 110 ppbv between 500 m and 2000 m above the altitude under inspection (500 m and 1500 m in the Antarctic, including the site at Davis).

The ozone tropopause can be less robust during stratosphere-troposphere exchange, however it is more robust than the lapse rate tropopause at polar latitudes in winter and near jet streams in the lower stratosphere due to temperature inversions near the tropopause definition region [Bethan et al., 1996, Tomikawa et al., 2009, Alexander et al., 2013]. In this work the lower of these two tropopause altitudes is used, as both are calculated for each ozonesonde release. Here, we calculate both tropopause heights for each ozonesonde release and use whichever is lower. This choice avoids occasional unrealistically high tropopause heights due to perturbed ozone or temperature measurements in the ozonesonde data.

Figure 1 shows the monthly mean tropopause altitudes at each location (solid lines). The dashed lines in Figure 1 show the mean tropopause altitude calculated from the subset of ozonesondes that detected an STT event. The seasonal cycle in tropopause altitude at Melbourne is exhibited, showing a maximum in summer, and a minimum is winter. This cycle is much more sublte at Macquarie, and almost reversed at Davis, which has a minimum during autumn and maximum from winter to spring. The decreasing tropopause altitude which occurs at higher southern latitudes is also apparent, as lower mean tropopause heights occur with more southern latitudes. The tropopause is higher on days with an STT event at all during winter and sprint at Davis.

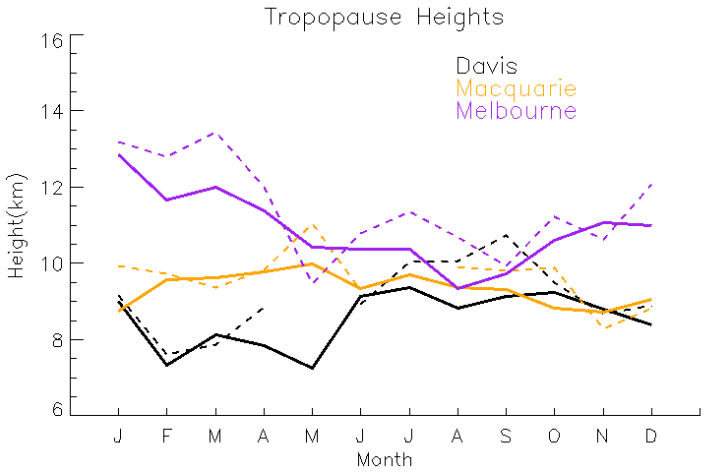

Figure 1: Multi-year monthly mean tropopause altitude (minimum of lapse rate and ozone defined tropopause) determined from ozonesondes measurements at Melbourne (2004-2013), Macquarie (2004-2013) and Davis (2006-2013) (solid lines). Dashed lines show the monthly mean tropopause altitude for the subset of dates when STT events occurred. (TODO: vertical shaded 90th percentiles, change height lable to altitude)

Figure 2 shows multi-year averaged ozone mixing ratios measured by ozonesonde over the three stations. Over Melbourne, increased ozone extending down through the troposphere is apparent from December to March and September to November. The increased tropospheric ozone in these months are due to STTs (in summer), and possible fire smoke plume influence (in winter), discussed in more detail below. Over Davis and Macquarie Island, the tropospheric ozone is higher between March and October, although the seasonal differences are small compared to those at Melbourne. This seasonality at the high latitude sites is driven by a decrease in photochemical destruction when the solar zenith angle is greater, causing light to have longer path length and reduced radiation (TODO: read and cite S. Oltmans antarctic papers - re Andrews comment).

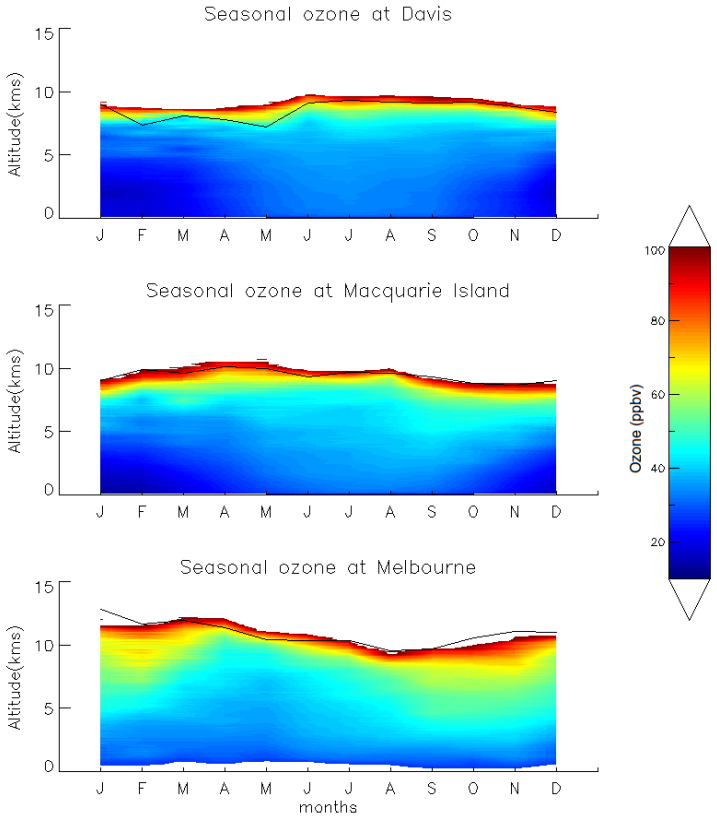

Figure 2: Multi-year mean seasonal cycle of ozone mixing ratio over Davis, Macquarie, and Melbourne measured by ozonesondes. Measurements were binned monthly and interpolated between months. Black solid lines show mean tropopause altitudes, defined as described in the text.

2.2 Characterisation of STT events and associated fluxes

We characterise STT events using the ozonesonde vertical profiles to identify tropospheric ozone volume mixing ratio enhancements above a local background (in moles per billion moles of dry air, or ppb). Calculation of ozone transport is performed after converting the profile to molecules cm^{-3}. The process is illustrated in Figure 3 for an example ozone profile.

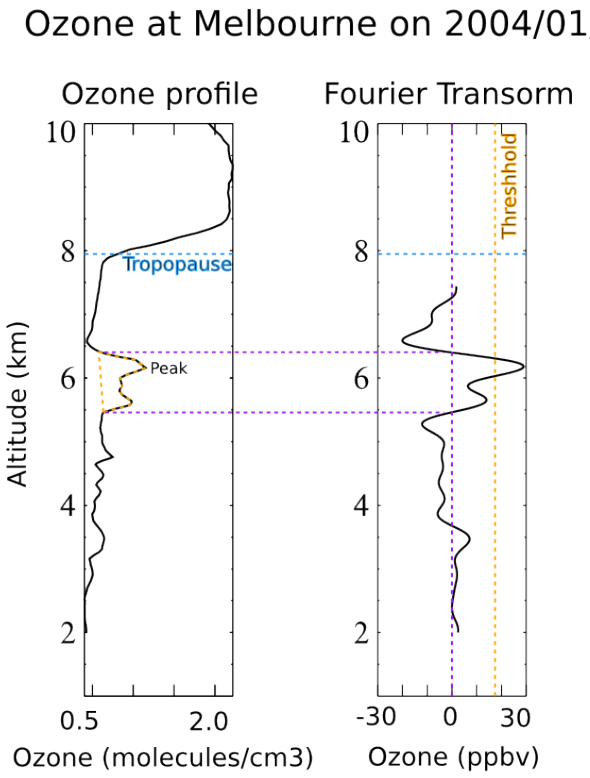

Figure 3: An example of the STT identification and flux estimation methods used in this work. The left panel shows an ozone mixing ratio profile from Melbourne on the 8th of January 2004 from 2km to the tropopause (dashed horizontal line). The right panel shows the perturbation profile created from bandpass filtering of the mixing ratio profile. The STT occurrence threshold calculated from the 99th percentile of filtered ozone perturbations is shown with the orange dashed line, and the technique for determining the vertical extent of the event is shown with the purple dashed lines (see details in text). The ozone flux associated with the STT event is calculated using the area outlined with the orange dashed line in the left panel.

First, the ozone vertical profiles are linearly interpolated to a regular grid with 20 m resolution from the surface to 14 km altitude. The interpolated profiles are then bandpass filtered using a Fourier transform to retain perturbations with vertical scales between 0.5 km and 5 km (removing low and high frequency perturbations). In what follows, these filtered vertical profiles are referred to as perturbation profiles. The choice of band limits was set empirically. For an event to qualify as STT, a clear increase above the background ozone level is needed, and we find that a vertical limit of $\sim$ 5 km removes seasonal-scale effects. The 0.5 km scale limit is set in order to remove any spikes of ozone which could be considered noise. We next use all the perturbation profiles at each site to calculate the 99th percentile perturbation value for the site. This is considered our threshold for tropospheric ozone perturbations, and perturbations above this threshold in individual ozonesondes are classified as STT events.

STTs which occur at altitudes below 4 km are removed in order to avoid surface pollution events Those occurring within 0.5 km of the tropopause are also removed in order to avoid spurious false positives induced by the sharp transition to stratospheric air.

Finally, we define the ozone peak as the altitude where the OMR is greatest within the lowest range of altitudes where the perturbation profile exceeds the percentile-based threshold. If the perturbation profile drops below zero between the ozone peak and the tropopause, the STT event is confirmed. Alternatively, if the OMR between the ozone peak and the tropopause drops below 80 ppb and is at least 20 ppb lower than the OMR at the ozone peak, the STT event is also confirmed. Otherwise the profile is rejected as a non-event. This final step removes near-tropopause anomalies for which there is no evidence of detachment from the stratosphere.

We estimate the ozone flux into the troposphere associated with each event by integrating the ozone concentration enhancement vertically over the altitude range for which an STT event is identified (i.e. the range surrounding the ozone peak over which the perturbation profile is greater than zero). This estimate is conservative because it does not take into any secondary ozone enhancements that may have been caused by the STT, and also ignores any heightened ozone background levels which may be due to synoptic-scale stratospheric mixing into the troposphere.

Tang and Prather [2010] define one possible method for detecting STT events from ozonesonde measurements. Their definition is based on subjective analysis of sondes released from 20 stations in the latitudinal range from 35°S to 40°N. In their work, a tropopause fold has occurred if, starting from 5 km altitude, the ozone level exceeds 80 ppb and then within 3 km decreases by 20 ppb or more to a value less than 120 ppb.

2.3 Biomass burning influenced events

The STT detection algorithm described in Section 2.2 assumes all mid-upper troposphere ozone perturbations above the 99th percentile are caused by stratospheric intrusions. In some cases, however, these perturbations may in fact re-

flect ozone production in lofted smoke plumes. Biomass burning in southern Africa and South America has previously been shown to have a major influence on atmospheric composition in the vicinity of our measurement sites [Gloudemans et al., 2007, Edwards et al., 2006], particularly from July to December [Pak et al., 2003]. On occasion, Australian and Indonesian fires can also reach the mid-high southern latitudes (TODO: cite this). TODO: Up to here with Jenny's Comments(done the sensitivities things though)

Ozone production from biomass burning is complex and affected by photochemistry, fuel nitrogen load, time since emission, and atmospheric plume chemistry both during transport and at the point of measurement. Large biomass burning events emit substantial ozone precursors, some of which are capable of being transported far from their origins. Peroxyacetyl Nitrate (PAN) is a reservoir of NO_x which can lead to enhanced ozone far from the source of a fire [Jaffe and Wigder, 2012].

Biomass burning influence in the Southern Hemisphere comes mostly from Southern Africa and South America, however Australian fires from the mid-latitudes, and Indonesian fires can also influence the ozonesonde release sites. Transported biomass burning plumes influence the southern mid-latitudes generally between July and December [Pak et al., 2003]. Biomass burning smoke plumes can lead to enhanced ozone, however this is not always the case. Due to the chance of smoke plume influence on STT characterisation, events which occur near smoke plumes are flagged and not included in STT flux calculations.

Removal of any possible influence from biomass burning smoke plumes is performed by detection of smoke plumes through global CO measurements. Here we identify transported smoke plumes through enhanced carbon monoxide (CO) levels. CO has a long enough lifetime to be an effective tracer of transport. The primary source of atmospheric enhancement of CO is fires, making CO a good indicator of fire plumes. Using high CO levels as a proxy for smoke plumes is a well established method (eg: Edwards [2003], Sinha et al. [2004], Edwards et al. [2006], Mari et al. [2008]). We use data from the AIRS (Atmospheric Infrared Sounder) instrument on board the Aqua satellite [AIR, 2013]. A visual inspection of AIRS' vertical columns of CO over the Southern Hemisphere is performed in order to exclude events with possible smoke influence at our three sites. We diagnose smoke plumes where high ($\sim 2 \times 10^{18}$ molecules cm^{-2} or higher) CO columns appear and when these occur near our sites during a sonde-detected ozone event, the event is flagged.

Figure 4(top) shows a day where smoke plumes are near the Melbourne sonde launch site on the day of a detected event. An event preliminarily detected on this day through the ozonesonde data is flagged as possibly due to fire. In the figure elevated CO levels can be seen over Australia, likely due to long-range transport from African and/or South American biomass burning. This day can be contrasted with the example in figure 4(bottom) where low CO levels are observed over the entire Southern Hemisphere. We screened all days at all three sites where an STT event is detected except for one event that coincided with missing AIRS data (January 2010). We flagged 15 of 72 events over Melbourne, 8 of 48 events over Macquarie island, and none from 45 over Davis. Nearly all of

the flagged events occur within the burning season of the Southern Hemisphere.

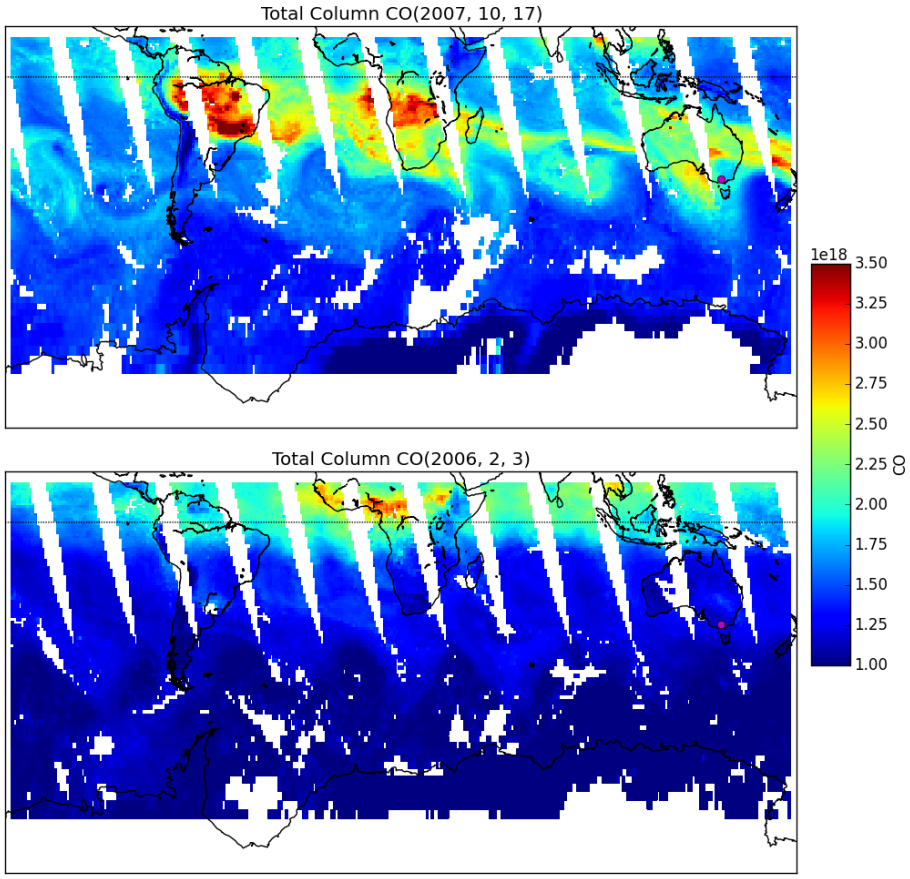

Figure 4: AIRS total column CO. The top panel (17 October 2007) is a day when ozone above Melbourne (purple dot) could have been caused by a transported biomass burning plume, and so was excluded from analysis. The bottom panel (3 February 2006) shows an example of a day when Melbourne ozone was likely not influenced by transported smoke plumes and was retained for analysis.

STT events flagged in this way are included in Figures 7 to 9, they are coloured red and do not contribute to STT flux calculations. These flagged events are concentrated in spring at Melbourne and Macquarie Island, and don't have any otherwise notable characteristics.

2.4 Sensitivities and limitations

Our method uses several subjectively defined quantities in the process of STT event detection. Here we briefly discuss these and the sensitivity to each. Using

the algorithm discussed in section 2.2, we detect 45 events at Davis, 47 (+8 fire influenced) events at Macquarie Island, and 72(+14 fire influenced) events at Melbourne.

The cut-off threshold (defined separately for each site) is determined from the 99th percentile of the ozone perturbations between 2 km and 1 km below the tropopause. We use the 99th percentile because at this point the filter locates clear events with no obvious false positives. Event detection is highly sensitive to this choice; for example, using the 98.5th percentile instead increased detected events by 24 at Melbourne (33%), 19 at Macquarie Island (40%), and 10 at Davis (22%). This high sensitivity means that detection is also sensitive to the profile altitude bounds used in calculation of the percentiles, i.e. the 2 km altitude to 1 km below the tropopause range. The altitude range used to determine the 99th percentile is set from 2 km up to 1 km below the tropopause. This range removes any anomalous edge effects of the Fourier bandpass filter, as well as discounting the highly variable ozone concentration which occurs near the tropopause. Finally, ozone enhancements are only considered STT events if they occur above 4 km and within 500 m below the tropopause. This range removes possible ground pollution, as well as allowing event detection up to 500 m from the tropopause. Some events, including the storm-caused event examined in figure 5 are within one kilometer of the tropopause.

TODO: Check and mention bandpass scale sensitivity.

3 Case Studies of synoptic conditions during STT events

We examine two case studies in detail to illustrate the synoptic-scale conditions in which STT events occur over Melbourne. Data from the European Center for Medium-range Weather Forecasts (ECMWF) Interim Reanalysis (ERA-I) [Dee et al., 2011] product is used for synoptic-scale examination of weather patterns over our three sites on dates matching detected STT events.

Figure 5(left) shows the ozonesonde profile recorded on the 3rd of February 2005 above Melbourne. Both tropopause definitions are between 400 and 500 hPa and the ozone spikes have clear anticorrelations with the relative humidity, suggesting dry stratospheric air is measured here. An ozone intrusion into the troposphere is identified by our detection algorithm at $\sim$ 520 hPa. Figure 5(right) shows the synoptic weather system, a cut-off low pressure system which caused a large storm and lowered the local tropopause height for several days. The wind circles around the low pressure system in a clockwise direction, typical geostrophic flows which are caused by pressure gradients and coriolis forces. The flux of stratospheric ozone brought into the troposphere by this event is at least 3.1×10^{11} molecules cm^{-3} , or 8% of the tropospheric ozone column.

Figure 6(left) shows the vertical ozonesonde profile recorded on the 13th January 2010 over Melbourne. The tropopause heights are greater at this time and an ozone intrusion is identified centred around 200 hPa. Again, anticorre-

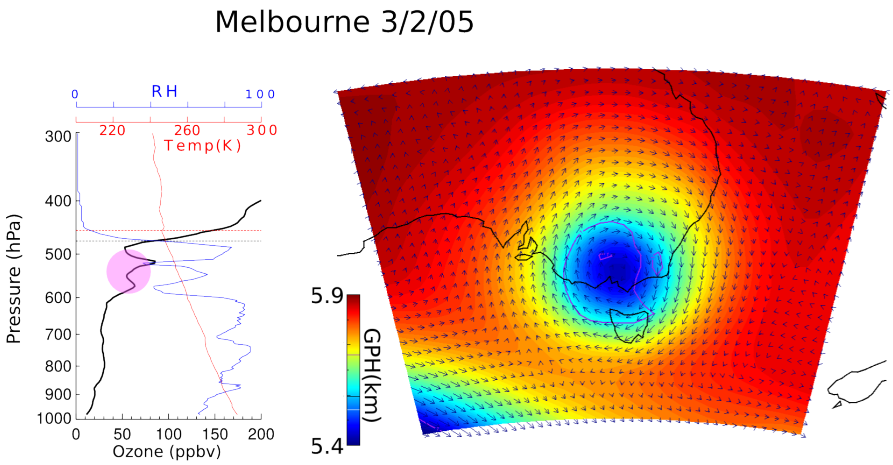

Figure 5: (Left) Vertical profile of ozone (black line), relative humidity (blue line), and temperature (red line) for 3 February 2005. The STT ozone event is highlighted in pink. The tropopause heights using both the ozone definition (black dashed line) and lapse rate definition (red dashed line) are shown. (Right) Synoptic weather map at 500 hPa from the ERA-Interim reanalysis. Vectors show wind direction and speed while colour indicates the geopotential height. Also visible are contours of potential vorticity units with 1 PVU in purple.

lated relative humidity provides evidence that the air is stratospheric in origin. Note the separation between this intrusion and the ozone tropopause (marked by the black dashed line), which indicates that the sonde passes through regular tropospheric air after hitting a stratospheric intrusion but before reaching the tropopause. Figure 6(right) shows a trough of low pressure (a low pressure front) passing over south-eastern Australia. This low pressure system crosses west to east and causes a wave of lowered tropopause height, which is often the cause of stratospheric mixing. During frontal passage, stratospheric air descends and streamers of ozone-rich air break off and mix into the troposphere [Sprenger et al., 2003].

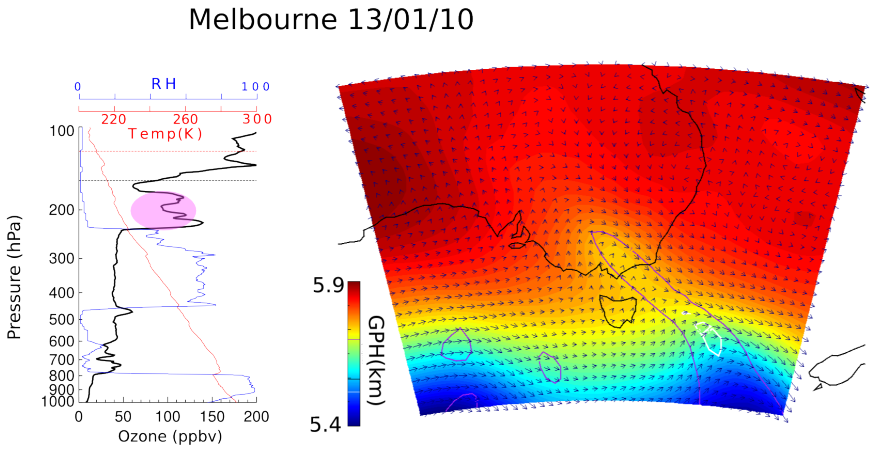

Figure 6: As figure 5, for 13 January 2010. Additionally visible is a 2 PVU contour, often used to determine dynamical tropopause height, in white.

An investigation of the ERA-I synoptic weather during STT events above Melbourne, Macquarie Island, and Davis are performed and are used to subjectively classify the events based on their likely cause. Similar characteristics to the case studies presented here occur over Macquarie Island: i.e. a prevalence of frontal and low pressure activity during STT events. Typically during STT occurrence, the upper troposphere is not calm, with low pressure fronts or cutoffs nearby at coincident time. Over Davis the weather systems are harder to distinguish, and the stratospheric polar vortex may create ozone folds without other sources of upper tropospheric turbulence.

4 STT event climatologies

Figure 7 shows the seasonal cycles of the STT events for Melbourne, Macquarie Island, and Davis. There is an annual cycle with a summertime peak

in the frequency of STT events above Melbourne and Macquarie Island. This summertime peak is due to a prevalence of summer storms, with low pressure systems bringing storms and turbulence along with a lowered tropopause level [Reutter et al., 2015].

A subjective analysis of ERA-I synoptic scale wind and altitude at 500 hPa over the three sites (eg: Figure 5(right)) leads to the categorisation of events based on their probable climatological cause. Probable causes are either low pressure fronts, low pressure cut-offs, or undetermined(misc). These categories are coloured as shades of blue in plots 7-9. This analysis suggests that low pressure cut-off systems are more prevalent in late summer at both Macquarie and Melbourne, and during winter at Davis.

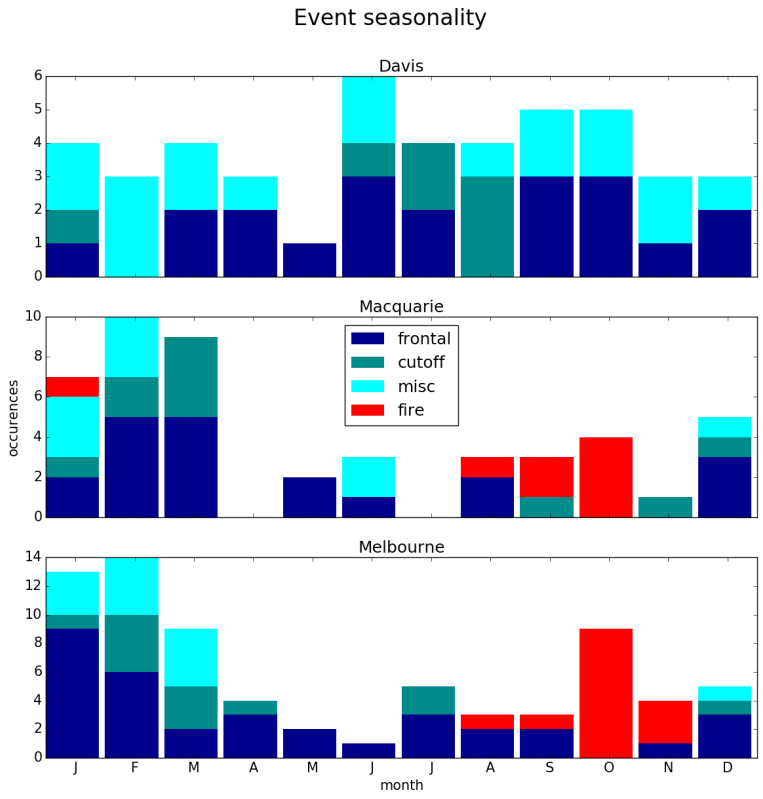

Figure 7: The seasonality of STT events at Davis, Macquarie Island, and Melbourne. Events are categorised by associated weather, and coloured bars from each category are stacked atop one another. The events filtered out as possibly smoke plume influenced are displayed here in red.

The frequency of STT events above Davis is relatively constant throughout the year, with a slight increase in events during antarctic winter. The slightly increased winter time frequency may be attributable to the increased frequency of sonde releases during the June to October months over Davis. It could be that events are non-seasonal at Davis, or else that the sample of 45 detected events over 10 years is too small or sparse to clearly show any cycle. It is possible that summer events caused by upper troposphere turbulence are balanced out by the events caused by the polar front jet stream, which is strongest during antarctic winter. The polar front jet stream is a band of wind extending from the mid troposphere up to the lower stratosphere, which is generally active from winter to spring. This vortex may be directly causing or impacting many of the STTs due to the lowered tropopause altitude which occurs south of the vortex edge (around 60°S).

Figure 8 shows the altitudes of detected events, based on the peak (maximum) of tropospheric ozone. STT event peaks most commonly occur at 6 – 10 km above Melbourne and below 8 km at Davis but are distributed more evenly at Macquarie Island, up to 7.5 kilometres altitude. Figure 9 shows the depths of detected events, based on the ozone peak's distance from the minimal determined tropopause. The majority of event peaks occur within 3 km of the tropopause at both Melbourne and Macquarie Island, and within 2 km of the tropopause at Davis.

For both Melbourne and Macquarie Island, the STT events which are unlikely to be fire-related occur mostly in summer and mostly during low pressure synoptic systems which can increase convection and upper tropospheric turbulence.

5 Comparison with GEOS-Chem

GEOS-Chem is a global chemical transport model [Bey et al., 2001], which includes transport, emission, deposition, chemical production and destruction of ozone and 103 other trace gases throughout the troposphere along with stratospheric chemistry, including photolysis. Stratosphere-troposphere coupling is calculated using the stratospheric unified chemistry extension (UCX) [Eastham et al., 2014], which includes a further 28 trace gases. For comparison to ozonesonde observations, we use GEOS-Chem version 10-011 (including UCX) run from 2005-2012, following a 1-year spin-up for 2004. Transport is driven by assimilated meteorological fields from the Goddard Earth Observing System (GEOS-5) maintained by the Global Modeling and Assimilation Office (GMAO) at NASA. Our simulation was modified from the standard v10-01 to a fix a bug in the treatment of the Total Ozone Mapping Spectrometer (TOMS) satellite data used to calculate photolysis (see Henderson [2016]). The simulation uses 2° latitude by 2.5° longitude horizontal resolution, with 72 vertical levels from the surface to 0.1 hPa. Biogenic emissions of organic chemicals are determined by the Model of Emissions of Gases and Aerosols from Nature (MEGAN) version 2.1 extended by Guenther et al [Guenther et al., 2012]. Anthropogenic emis-

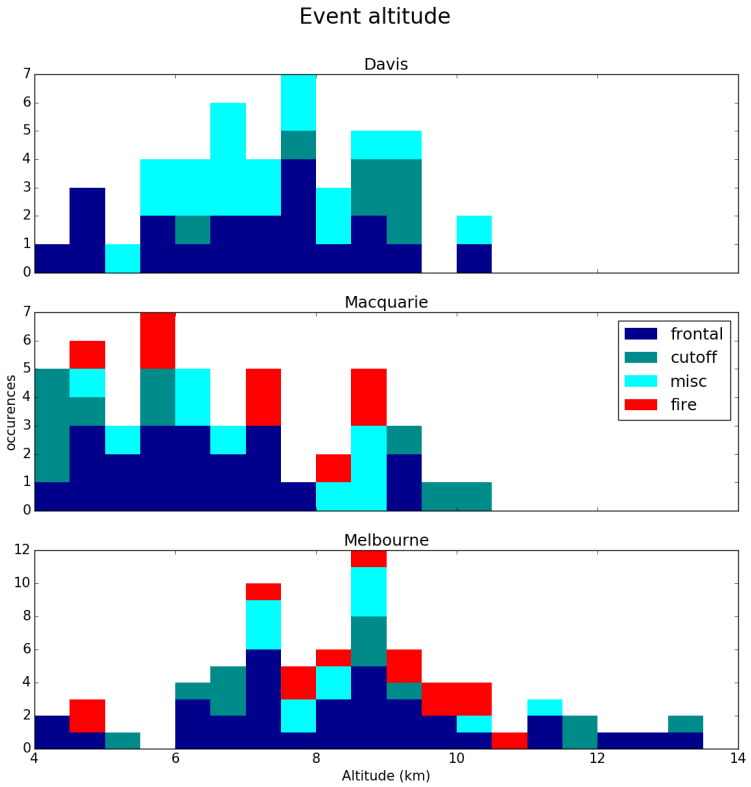

Figure 8: The distribution of the ozone peak altitude for Davis, Macquarie Island, and Melbourne. This shows the altitude of detected events, based on the tropospheric ozone enhancement peak. Events are categorised by likely causes, with possible smoke influenced events displayed in red.

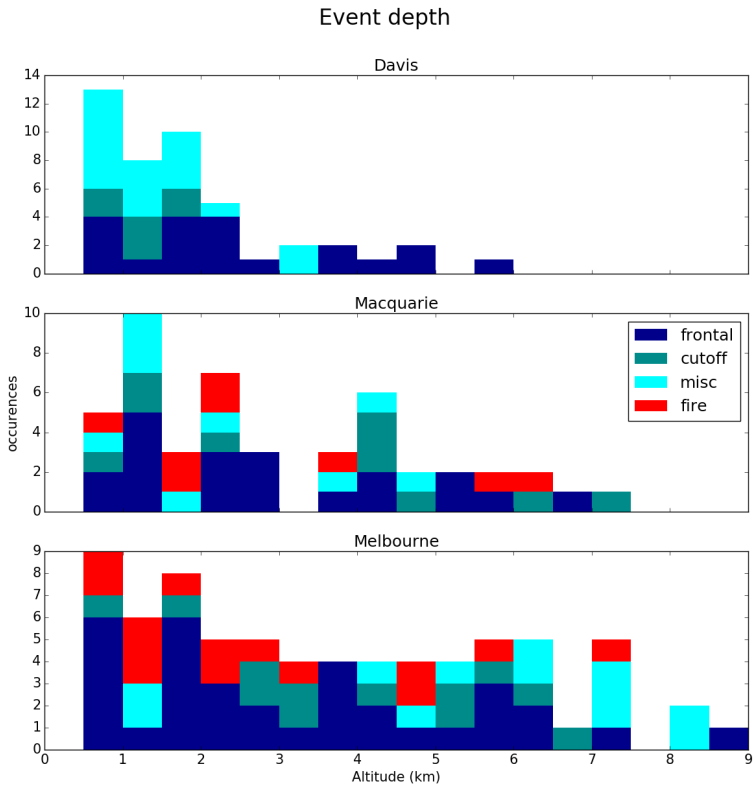

Figure 9: The distance between the ozone peak and the tropopause, and the cumulative probability of these distances (blue line) for Davis, Macquarie Island, and Melbourne. This shows the depth of the event into the troposphere, starting from the tropopause. The events filtered out as possibly smoke plume influenced are displayed here in red.

sions are given by the Emissions Database for Global Atmospheric Research (EDGAR) version 4.2.

Ozonesondes are useful for looking at specific locations with high resolution, and in this work they provide an estimate of both STT occurence rates and STT ozone flux. At these discrete locations, this information can be used in conjunction with global-scale information in order to quantify ozone transport over a large area. GEOS-Chem is used to simulate the global ozone concentrations. In order to check that the model is reasonable, some simple validation is performed. Comparisons of both ozonesonde and GEOS-Chem simulated tropospheric ozone profiles and partial columns are checked, averaging seasonally for colocated data. Following this, an extrapolation is performed and the stratospherically sourced ozone is estimated over the latitude range from 35°S to 75°S. This range is used as it includes all three sites, a change of 5° in either direction at either end of the range changes the average tropospheric ozone by -8 to 9%. Examination of the GEOS-Chem output also gives us an insight as to whether the simulation can be used on its own in order to estimate STT event distribution and magnitude.

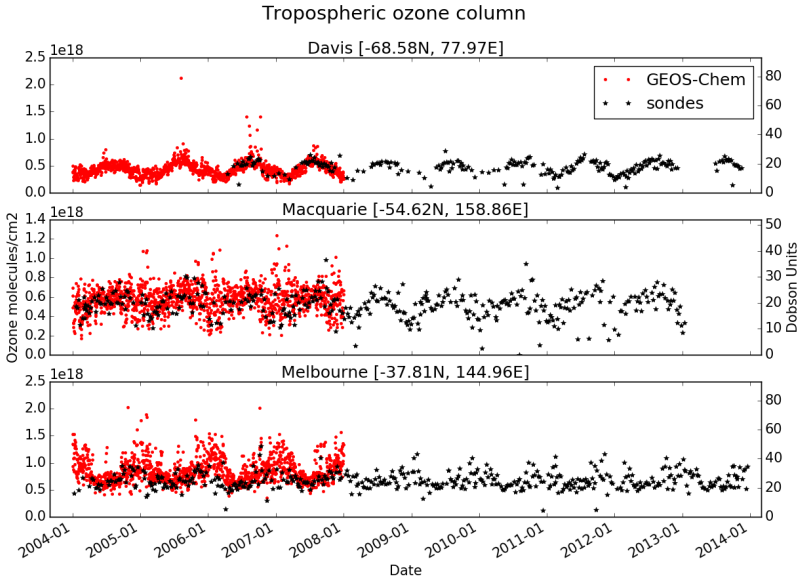

Figure 10: Tropospheric ozone column (Ω_{O3}, in molecules cm^{-2}) at daily resolution simulated by GEOS-Chem (red dots) from January 1 2004 to December 31 2013. The GEOS-Chem datapoints are respectively at 7AM, 11AM, and 11AM for Davis, Macquarie, and Melbourne. Columns calculated from ozonesondes are shown as black stars, each representing one measurement. (TODO: Update once fixed model run finishes)

Figure 10 compares the time series of tropospheric ozone column (Ω_{O_3}) in molecules cm^{-2} simulated by GEOS-Chem (red dots) to the measured tropospheric ozone columns (black stars). Sonde tropospheric columns are calculated using the GPH and ozone partial pressure recorded by the ozonesondes, using TODO: equation here. The seasonal cycles are well correlated, with similar timing and magnitude (paired r^2 values of TODO: run script when model run finished). The maximum ozone column at Melbourne occurs in summer, with a minimum in winter. Macquarie and Davis show the opposite seasonal cycle. The model shows more spread than the ozonesondes, although there are daily simulated values for the model while only weekly or less for the ozonesondes.

Figure 11 shows the measured and simulated seasonal mean ozone profile at all sites. The model generally underestimates ozone at low altitudes (up to 6 km) at both Davis and Macquarie, although this is less pronounced during summer. Over Melbourne an opposite bias is seen, where the model shows increased ozone levels from around 4 km up to the tropopause. Also notable is the lower tropopause height exhibited by the model, which on average is lower by $\sim$ 1 km (TODO: mean bias, updated when model finishes). The effect of pollution and mainland influence can be seen over Melbourne, mostly during the summer months (DJF), as the lower altitudes have increased ozone mean as well as more variance

Although GEOS-Chem reasonably matches the ozonesonde tropospheric ozone column, it does not have the resolution required to capture STTs. Figure 12 shows the best (left) and worst (right) comparisons of ozone profiles up to 14 km between the ozonesondes and GEOS-Chem. The model output is shown in red, and is the average over 2° latitude by 2.5° longitude which contain the respective sonde release site. The vertical resolution from GEOS-Chem is too low to allow detection of STTs, with roughly 30 vertical levels up to the tropopause, while sondes have upwards of 100.

6 Stratosphere to troposphere ozone flux from STT events

Based on the integrated ozone amount associated with each STT event (see section 2.2), we find a lower bound for the STT ozone flux over each of our three sites (fire influence excluded). This is a conservative lower bound as the algorithm ignores secondary ozone peaks which may also be transported down from the stratosphere, as well as ignoring potential ozone dispersion from the ozone peak. Figure 13 shows the mean fraction of total tropospheric column ozone attributed to stratospheric ozone intrusions at each site, averaged over days when an STT event occurs. The mean fraction of tropospheric ozone attributed to STT events is 2–4%, on individual days this value can exceed 10% at Macquarie and Melbourne. Figure 14 shows the data in absolute terms, and indicates that the mean STT event impact is around 1 to 2×10^{16} molecules/cm^2. Our flux estimates are relatively insensitive to our biomass burning filter; including

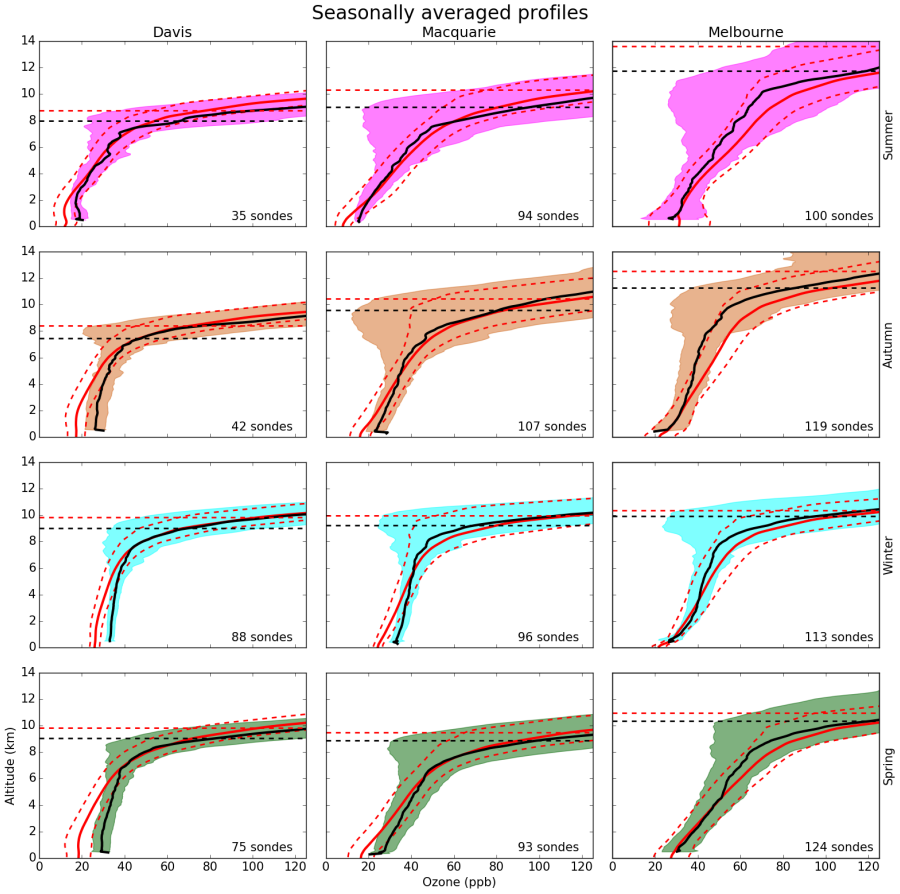

Figure 11: Tropospheric ozone (ppb) over Davis, Macquarie, and Melbourne, seasonally averaged. GEOS-Chem simulated data averaged over January 2005 until December 2013 are shown with red lines, with dashed red lines showing one standard deviation. Ozonesonde measurements are shown with black lines, and have seasonally coloured shaded areas over the mean plus or minus one standard deviation. Horizontal dotted line shows the mean tropopause heights, again red for the GEOS-Chem simulation and black for ozonesondes. TODO: Update once fixed model run finishes.

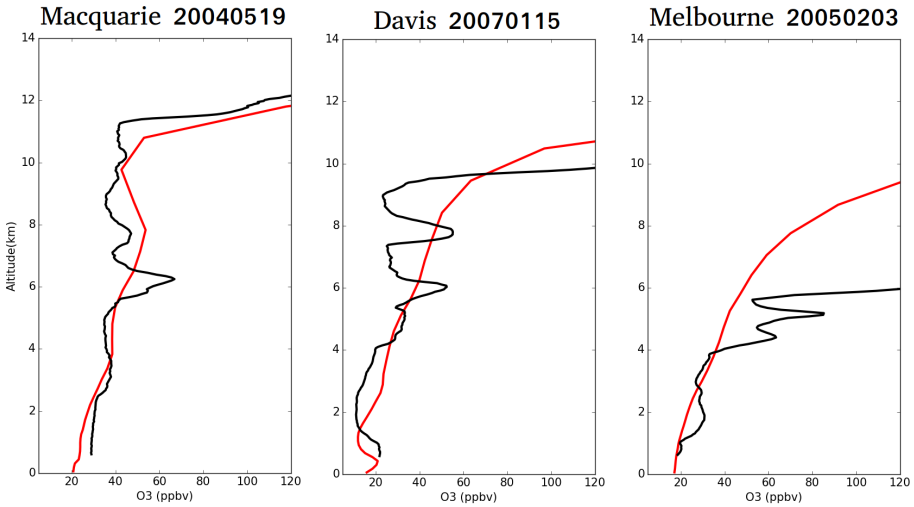

Figure 12: Ozonesonde profiles (black) against GEOS-Chem profiles (red) for three different dates, one over each site. The dates were picked based on subjective visual analysis as follows: left is the best match - May 19th 2004 over Macquarie, middle is an average case - January 15th, 2007 over Davis, and right is the worst match - February 3rd 2005 over Melbourne.

smoke-influenced days changes the mean flux by less than 0.25% (5% relative change).

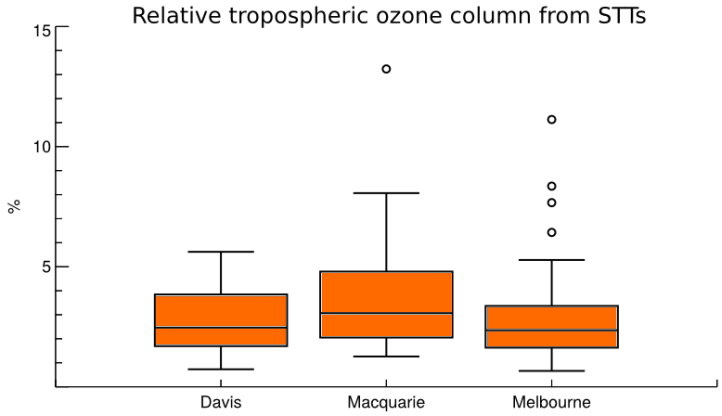

Figure 13: Fraction of total tropospheric column ozone attributed to stratospheric air intrusions during STT events.

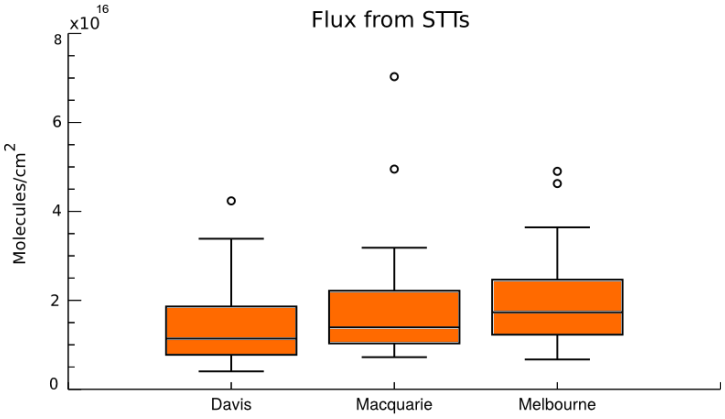

Figure 14: Tropospheric ozone attributed to stratospheric air intrusions during STT events.

Extrapolating out over the Southern Ocean using our estimated enhanced tropospheric ozone, we can create a rough estimate of the STT effect on tropospheric ozone in this region. This is be done by multiplying the monthly likelihoods of STTs with the monthly tropospheric column ozone amounts multiplied by our mean flux fraction. Taking the monthly likelihood from our ozonesonde events count per sondes released during each month, and southern latitude tropospheric column ozone amount from GEOS-Chem, the total amount of ozone from STT events over the southern ocean is at least (TODO:update once fixed model is finished) 2.2×10^{16} molecules cm^{-2} yr^{-1}, TODO: this is around X:TG/yr ozone. Figure 15 shows the seasonal STT contribution calculated this way, with 'l' and 'f' being the STT likelihood and fraction respectively.

Our estimate is (todo: greater/smaller/completely different) to other estimates of southern hemispheric ozone transport. Olsen [2003] use PV and winds from GEOS along with ozone measurements from TOMS to estimate that around 210 TG yr^{-1} of ozone flux occurs in 2000 between 30°S and 60°S. Their estimates show a peak in flux from winter to early spring (JJAS), which is the same months when our GEOS-Chem simulation shows the highest tropospheric Ω_{O3}. Global STT flux estimated from an ensemble of models shows global STT flux at around 550 Tg yr^{-1} [Stevenson et al., 2006]. Global net flux (transport from the stratosphere to the troposphere minus opposite transport) is estimated to be 75 Tg yr^{-1} [Sprenger et al., 2003].

Considering the individual event contributions, Terao et al. [2008] estimate much higher STT impacts; where 30–40% of the tropospheric column is due to STT. Although this figure is based on the Northern Hemisphere during the seasonal STT peak.

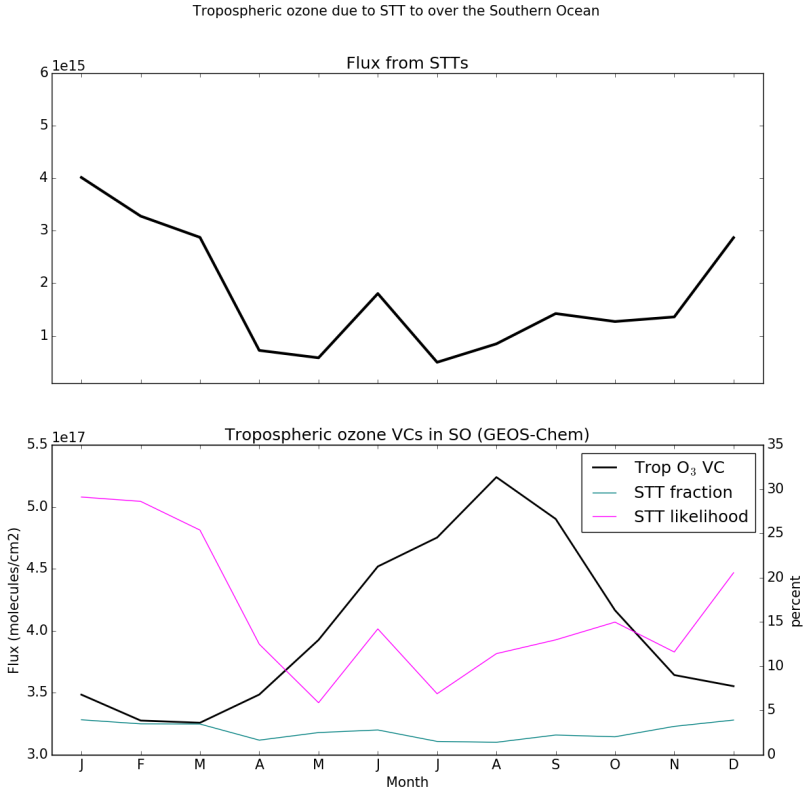

Figure 15: Top panel shows the estimated STT contribution to tropospheric ozone VC. Bottom panel shows the three factors multiplied together in order to produce the estimation. Units for 'l' and 'f' are on the right, while units for ozone VC amounts are on the left.

7 Conclusions

Ozonesonde data in the Southern Hemisphere provides a satellite-independant quantification of STT ozone transport. The frequency and amount of ozone descending from the stratosphere into the troposphere can be estimated from the long time series of tropospheric ozone profiles. Using almost ten years of ozonesonde profiles over the southern high latitudes, a clear summer peak is seen for STT occurences at both 38°S and 55°S, although not at 69°S.

We use a Fourier bandpass filter to determine STT ozone transport events. The filter removes seasonal tropospheric ozone influences and allows clear detection of ozone-enhanced tongues of air in the troposphere. By setting empirical checks, ozonesonde vertical profiles can clearly show tropospheric ozone enhancement which is separated from the stratosphere. The cause of these ozone enhancements is examined through the use of satellite and reanalysis datasets on case studies above Melbourne. The major causes of STT events found over Melbourne are turbulent weather in the upper troposphere due to low pressure fronts and cut-off low pressure systems. TODO: Discuss Davis,Macq here

Integration of the ozone enhancement along the altitude of the ozone profile allows a rough estimate of stratospheric transport for each event. Events typically cause a 3% enhancement of the tropospheric ozone column. This is around 2×10^{15} molecules cm^{-2} (TODO: Update when model run finishes) ozone enhancement over the southern high latitudes caused by STTs.

GEOS-Chem performs fairly well when compared to ozonesondes at our three sites, with vertical profile averages and seasonal cycles of tropospheric ozone conforming to within $\sim 10\%$ (TODO: update when model finishes) of the data, even though the model is looking at the average over 2° latitude by 2.5° longitude grid boxes.

References

AIRS3STD, 2013.

S. P. Alexander, D. J. Murphy, and A. R. Klekociuk. High resolution VHF radar measurements of tropopause structure and variability at Davis, Antarctica (69?? S, 78?? E). *Atmospheric Chemistry and Physics*, 13(6):3121–3132, 2013. ISSN 16807324. doi: 10.5194/acp-13-3121-2013. URL `http://www.atmos-chem-phys.net/13/3121/2013/`.

Shiri Avnery, Denise L. Mauzerall, Junfeng Liu, and Larry W. Horowitz. Global crop yield reductions due to surface ozone exposure: 2. Year 2030 potential crop production losses and economic damage under two scenarios of O 3 pollution. *Atmospheric Environment*, 71(13):408–409, 2013. ISSN 13522310. doi: 10.1016/j.atmosenv.2012.12.045. URL `http://dx.doi.org/10.1016/j.atmosenv.2011.01.002`.

J. L. Baray, V. Daniel, G. Ancellet, and B. Legras. Planetary-scale tropopause

folds in the southern subtropics. *Geophysical Research Letters*, 27(3):353–356, 2000. ISSN 00948276. doi: 10.1029/1999GL010788.

M. Beekmann, G. Ancellet, S. Blonsky, D. De Muer, A. Ebel, H. Elbern, J. Hendricks, J. Kowol, C. Mancier, R. Sladkovic, H. G J Smit, P. Speth, T. Trickl, and Ph Van Haver. Regional and global tropopause fold occurrence and related ozone flux across the tropopause. *Journal of Atmospheric Chemistry*, 28(1-3):29–44, 1997. ISSN 01677764. doi: 10.1023/A:1005897314623.

S. Bethan, G. Vaughan, and S. J. Reid. A comparison of ozone and thermal tropopause heights and the impact of tropopause definition on quantifying the ozone content of the troposphere. *Quarterly Journal of the Royal Meteorological Society*, 122(532):929–944, 1996. ISSN 00359009. doi: 10.1002/qj.49712253207. URL `http://doi.wiley.com/10.1002/qj.49712253207`.

Isabelle Bey, Daniel J. Jacob, Robert M. Yantosca, Jennifer A. Logan, Brendan D. Field, Arlene M. Fiore, Qin-Bin Li, Hong-Yu Liu, Loretta J. Mickley, and Martin G. Schultz. Global Modeling of Tropospheric Chemistry with Assimilated Meteorology: Model Description and Evaluation. *Journal of Geophysical Research*, 106:73–95, 2001. ISSN 0148-0227. doi: 10.1029/2001JD000807.

Edwin F. Danielsen. Stratospheric-Tropospheric Exchange Based on Radioactivity, Ozone and Potential Vorticity, 1968. ISSN 0022-4928.

S S Das, M V Ratnam, K N Uma, K V Subrahmanyam, and I A Girach. Influence of tropical cyclones on tropospheric ozone : possible implication. *Atmospheric Chemistry and Physics (Discussions)*, 15(2003):19305–19323, 2016. ISSN 1680-7324. doi: 10.5194/acpd-15-19305-2015.

D P Dee, S M Uppala, A J Simmons, P Berrisford, P Poli, S Kobayashi, U Andrae, M A Balmaseda, G Balsamo, P Bauer, P Bechtold, A C M Beljaars, L van de Berg, J Bidlot, N Bormann, C Delsol, R Dragani, M Fuentes, A J Geer, L Haimberger, S B Healy, H Hersbach, E V HÃ³lm, L Isaksen, P KÃ¥llberg, M KÃ¶hler, M Matricardi, A P McNally, B M Monge-Sanz, J.-J. Morcrette, B.-K. Park, C Peubey, P de Rosnay, C Tavolato, J.-N. ThÃ©paut, and F Vitart. The ERA-Interim reanalysis: configuration and performance of the data assimilation system. *Quarterly Journal of the Royal Meteorological Society*, 137(656):553–597, 2011. ISSN 1477-870X. doi: 10.1002/qj.828. URL `http://dx.doi.org/10.1002/qj.828`.

Sebastian D. Eastham, Debra K. Weisenstein, and Steven R H Barrett. Development and evaluation of the unified tropospheric-stratospheric chemistry extension (UCX) for the global chemistry-transport model GEOS-Chem. *Atmospheric Environment*, 89:52–63, 2014. ISSN 13522310. doi: 10.1016/j.atmosenv.2014.02.001. URL `http://dx.doi.org/10.1016/j.atmosenv.2014.02.001`.

D. P. Edwards. Tropospheric ozone over the tropical Atlantic: A satellite perspective. *Journal of Geophysical Research*, 108(D8):4237, 2003. ISSN 0148-0227. doi: 10.1029/2002JD002927. URL http://doi.wiley.com/10.1029/2002JD002927.

D. P. Edwards, L. K. Emmons, J. C. Gille, A. Chu, J. L. Attié, L. Giglio, S. W. Wood, Jim Haywood, M. N. Deeter, S. T. Massie, D. C. Ziskin, and James R. Drummond. Satellite-observed pollution from Southern Hemisphere biomass burning. *Journal of Geophysical Research Atmospheres*, 111(14):1–17, 2006. ISSN 01480227. doi: 10.1029/2005JD006655.

P. Forster, V. Ramaswamy, P. Artaxo, T. Berntsen, R. Betts, D.W. Fahey, J. Haywood, J. Lean, D.C. Lowe, G. Myhre, J. Nganga, R. Prinn, G. Raga, M. Schulz, and R. Van Dorland. Changes in Atmospheric Constituents and in Radiative Forcing. In: Climate Change 2007: The Physical Science Basis. Contribution of Working Group I to the Fourth Assessment Report of the Intergovernmental Panel on Climate Change[Solomon, S., D. Qin, M. Man, 2007. URL https://www.ipcc.ch/publications_and_data/ar4/wg1/en/ch2.html.

W. Frey, R. Schofield, P. Hoor, D. Kunkel, F. Ravegnani, a. Ulanovsky, S. Viciani, F. D'Amato, and T. P. Lane. The impact of overshooting deep convection on local transport and mixing in the tropical upper troposphere/lower stratosphere (UTLS). *Atmospheric Chemistry and Physics*, 15 (11):6467–6486, 2015. ISSN 1680-7324. doi: 10.5194/acp-15-6467-2015. URL http://www.atmos-chem-phys.net/15/6467/2015/.

E. Galani. Observations of stratosphere-to-troposphere transport events over the eastern Mediterranean using a ground-based lidar system. *Journal of Geophysical Research*, 108(D12):1–10, 2003. ISSN 0148-0227. doi: 10.1029/2002JD002596. URL http://www.agu.org/pubs/crossref/2003/2002JD002596.shtml.

Annemieke Gloudemans, Jos De Laat, Maarten Krol, Jan Fokke Meirink, Guido Van Der Werf, Hans Schrijver, and Ilse Aben. Evidence for long-range transport of carbon monoxide in the Southern Hemisphere from SCIAMACHY observations. *European Space Agency, (Special Publication) ESA SP*, 33(SP-636):1–5, 2007. ISSN 03796566. doi: 10.1029/2006GL026804.

A. B. Guenther, X. Jiang, C. L. Heald, T. Sakulyanontvittaya, T. Duhl, L. K. Emmons, and X. Wang. The model of emissions of gases and aerosols from nature version 2.1 (MEGAN2.1): An extended and updated framework for modeling biogenic emissions. *Geoscientific Model Development*, 5(6):1471–1492, 2012. ISSN 1991959X. doi: 10.5194/gmd-5-1471-2012.

Ben Henderson. TOMS OH Fix, 2016. URL http://wiki.seas.harvard.edu/geos-chem/index.php/FAST-JX_v7.0_photolysis_mechanism#Fix_for_TOMS_to_address_strange_cycle_in_OH_output.

M C Jacobson and H Hansson. Organic atmospheric aerosols: Review and state of the science. *Reviews of Geophysics*, (38):267–294, 2000. ISSN 87551209. doi: 10.1029/1998RG000045.

Daniel a. Jaffe and Nicole L. Wigder. Ozone production from wildfires: A critical review. *Atmospheric Environment*, 51:1–10, 2012. ISSN 13522310. doi: 10.1016/j.atmosenv.2011.11.063. URL `http://dx.doi.org/10.1016/j.atmosenv.2011.11.063`.

A. O. Langford, J. Brioude, O. R. Cooper, C. J. Senff, R. J. Alvarez, R. M. Hardesty, B. J. Johnson, and S. J. Oltmans. Stratospheric influence on surface ozone in the Los Angeles area during late spring and early summer of 2010. *Journal of Geophysical Research Atmospheres*, 117(3):1–17, 2012. ISSN 01480227. doi: 10.1029/2011JD016766.

Allen S. Lefohn, Heini Wernli, Douglas Shadwick, Sebastian Limbach, Samuel J. Oltmans, and Melvyn Shapiro. The importance of stratospheric-tropospheric transport in affecting surface ozone concentrations in the western and northern tier of the United States. *Atmospheric Environment*, 45(28):4845–4857, 2011. ISSN 13522310. doi: 10.1016/j.atmosenv.2011.06.014. URL `http://dx.doi.org/10.1016/j.atmosenv.2011.06.014`.

Meiyun Lin, Arlene M. Fiore, Owen R. Cooper, Larry W. Horowitz, Andrew O. Langford, Hiram Levy, Bryan J. Johnson, Vaishali Naik, Samuel J. Oltmans, and Christoph J. Senff. Springtime high surface ozone events over the western United States: Quantifying the role of stratospheric intrusions. *Journal of Geophysical Research Atmospheres*, 117(19):1–20, 2012. ISSN 01480227. doi: 10.1029/2012JD018151.

Junhua Liu, Jose M. Rodriguez, Anne M. Thompson, Jennifer A. Logan, Anne R. Douglass, Mark A. Olsen, Stephen D. Steenrod, and Françoise Posny. Origins of tropospheric ozone interannual variation over Réunion: A model investigation. *Journal of Geophysical Research Atmospheres*, pages 1–19, 2015. doi: 10.1002/2015JD023981. URL `http://onlinelibrary.wiley.com/doi/10.1002/2015JD023981/abstract`.

C H Mari, G Cailley, L Corre, M Saunois, Atti´ E, J L, V Thouret, and A Stohl. Tracing biomass burning plumes from the Southern Hemisphere during the AMMA 2006 wet season experiment, Atmos. *Atmospheric Chemistry and Physics*, 8:3951–3961, 2008. ISSN 1680-7324. doi: 10.5194/acpd-7-17339-2007.

M Mihalikova, S Kirkwood, J Arnault, and D Mikhaylova. Observation of a tropopause fold by MARA VHF wind-profiler radar and ozonesonde at Wasa, Antarctica: comparison with ECMWF analysis and a WRF model simulation. *Annales Geophysicae*, 30(9):1411–1421, 2012. doi: 10.5194/angeo-30-1411-2012. URL `http://www.ann-geophys.net/30/1411/2012/`.

N. Mze, A. Hauchecorne, H. Bencherif, F. Dalaudier, and J. L. Bertaux. Climatology and comparison of ozone from ENVISAT/GOMOS and SHADOZ/balloon-sonde observations in the southern tropics. *Atmospheric Chemistry and Physics*, 10(16):8025–8035, 2010. ISSN 16807316. doi: 10.5194/acp-10-8025-2010.

NOAA. NOAA Ozone sondes appendix. URL `http://www.ndsc.ncep.noaa.gov/organize/protocols/appendix5/`.

Mark a. Olsen. A comparison of Northern and Southern Hemisphere cross-tropopause ozone flux. *Geophysical Research Letters*, 30(7):1412, 2003. ISSN 0094-8276. doi: 10.1029/2002GL016538. URL `http://doi.wiley.com/10.1029/2002GL016538`.

B.C.a Pak, R.L.b Langenfelds, S.A.b Young, R.J.b Francey, C.P.b Meyer, L.M.b Kivlighon, L.N.b Cooper, B.Lb Dunse, C.E.b Allison, L.P.b Steele, IE.b Galbally, and I.A.b Weeks. Measurements of biomass burning influences in the troposphere over southeast Australia during the SAFARI 2000 dry season campaign. *Journal of Geophysical Research D: Atmospheres*, 108(13):SAF 16–1 – SAF 16–10, 2003. ISSN 0148-0227. doi: 10.1029/2002JD002343. URL `http://www.scopus.com/inward/record.url?eid=2-s2.0-0742322536&partnerID=40&md5=cafaeef03b948fb456696583ed3ab9a5`.

J. D. Price and G. Vaughan. The potential for stratosphere-troposphere exchange in cut-off-low systems. *Quarterly Journal of the Royal Meteorological Society*, 119(510):343–365, 1993. doi: 10.1002/qj.49711951007. URL `http://onlinelibrary.wiley.com/doi/10.1002/qj.49711951007/abstract`.

P. Reutter, B. Škerlak, M. Sprenger, and H. Wernli. Stratosphere-troposphere exchange (STE) in the vicinity of North Atlantic cyclones. *Atmospheric Chemistry and Physics*, 15(19):10939–10953, 2015. ISSN 16807324. doi: 10.5194/acp-15-10939-2015.

N E Selin, S Wu, K M Nam, J M Reilly, S Paltsev, R G Prinn, and M D Webster. Global health and economic impacts of future ozone pollution. *Environmental Research Letters*, 4(4):044014, 2009. ISSN 1748-9326. doi: 10.1088/1748-9326/4/4/044014.

Parikhit Sinha, Lyatt Jaeglé, Peter V. Hobbs, and Qing Liang. Transport of biomass burning emissions from southern Africa. *Journal of Geophysical Research*, 109:D20204, 2004. ISSN 01480227. doi: 10.1029/2004JD005044.

Herman G J Smit, Wolfgang Straeter, Bryan J. Johnson, Samuel J. Oltmans, Jonathan Davies, David W. Tarasick, Bruno Hoegger, Rene Stubi, Francis J. Schmidlin, T. Northam, Anne M. Thompson, Jacquelyn C. Witte, Ian Boyd, and Françoise Posny. Assessment of the performance of ECC-ozonesondes under quasi-flight conditions in the environmental simulation chamber: Insights

from the Juelich Ozone Sonde Intercomparison Experiment (JOSIE). *Journal of Geophysical Research Atmospheres*, 112(19):1–18, 2007. ISSN 01480227. doi: 10.1029/2006JD007308.

Michael Sprenger, Mischa Croci Maspoli, and Heini Wernli. Tropopause folds and cross-tropopause exchange: A global investigation based upon ECMWF analyses for the time period March 2000 to February 2001. *Journal of Geophysical Research: Atmospheres*, 108(D12):n/a—-n/a, 2003. ISSN 2156-2202. doi: 10.1029/2002JD002587. URL `http://dx.doi.org/10.1029/2002JD002587`.

D S Stevenson, F J Dentener, M G Schultz, K Ellingsen, T P C van Noije, O Wild, G Zeng, M Amann, C S Atherton, N Bell, D J Bergmann, I Bey, T Butler, J Cofala, W J Collins, R G Derwent, R M Doherty, J Drevet, H J Eskes, A M Fiore, M Gauss, D A Hauglustaine, L W Horowitz, I S A Isaksen, M C Krol, J.-F. Lamarque, M G Lawrence, V Montanaro, J.-F. Müller, G Pitari, M J Prather, J A Pyle, S Rast, J M Rodriguez, M G Sanderson, N H Savage, D T Shindell, S E Strahan, K Sudo, and S Szopa. Multimodel ensemble simulations of present-day and near-future tropospheric ozone. *J. Geophys. Res.*, 111(D8), 2006. doi: 10.1029/2005jd006338. URL `http://dx.doi.org/10.1029/2005JD006338`.

Andreas Stohl, Heini Wernli, Paul James, Michel Bourqui, Caroline Forster, Mark A. Liniger, Petra Seibert, and Michael Sprenger. A new perspective of stratosphere-troposphere exchange. *Bulletin of the American Meteorological Society*, 84(11):1565–1573+1473, 2003. ISSN 00030007. doi: 10.1175/BAMS-84-11-1565.

Q. Tang and M. J. Prather. Correlating tropospheric column ozone with tropopause folds: The Aura-OMI satellite data. *Atmospheric Chemistry and Physics*, 10(19):9681–9688, 2010. ISSN 16807316. doi: 10.5194/acp-10-9681-2010.

Q. Tang and M. J. Prather. Five blind men and an elephant: can NASA Aura measurements quantify the stratosphere-troposphere exchange of ozone flux? *Atmospheric Chemistry and Physics*, 11(5):2357–2380, 2012. ISSN 16807316. doi: 10.5194/acp-12-2357-2012. URL `http://dx.doi.org/10.5194/acpd-11-26897-2011`.

Yukio Terao, Jennifer A Logan, Anne R Douglass, and Richard S Stolarski. Contribution of stratospheric ozone to the interannual variability of tropospheric ozone in the northern extratropics. *J. Geophys. Res.*, 113(D18), 2008. doi: 10.1029/2008jd009854. URL `http://dx.doi.org/10.1029/2008jd009854`.

A. M. Thompson, N. V. Balashov, J. C. Witte, J. G R Coetzee, V. Thouret, and F. Posny. Tropospheric ozone increases over the southern Africa region: Bellwether for rapid growth in Southern Hemisphere pollution? *Atmospheric Chemistry and Physics*, 14(18):9855–9869, 2014. ISSN 16807324. doi: 10.5194/acp-14-9855-2014.

Yoshihiro Tomikawa, Yashiro Nishimura, and Takashi Yamanouchi. Characteristics of Tropopause and Tropopause Inversion Layer in the Polar Region. *SOLA*, 5:141–144, 2009. doi: 10.2151/sola.2009-036. URL `http://dx.doi.org/10.2151/sola.2009-036`.

G Vaughan, J D Price, and A Howells. Transport into the troposphere in a tropopause fold. *Quarterly Journal of the Royal Meteorological Society*, 120 (518):1085–1103, 1993. ISSN 00359009. doi: 10.1002/qj.49712051814.

Volkmar Wirth. Diabatic heating in an axisymmetric cut-off cyclone and related stratosphere-troposphere exchange. *Quarterly Journal of the Royal Meteorological Society*, 121(521):127–147, 1995. ISSN 00359009. doi: 10.1002/qj.49712152107. URL `http://doi.wiley.com/10.1002/qj.49712152107`.

World Meteorological Organization WMO. Meteorology A Three-Dimensional Science. *Geneva, Second Session of the Commission for Aerology*, 4:134–138, 1957.

L Zhang, D J Jacob, X Yue, N V Downey, D A Wood, and D Blewitt. Sources contributing to background surface ozone in the US Intermountain West. *Atmos. Chem. Phys.*, 14(11):5295–5309, 2014. doi: 10.5194/acp-14-5295-2014. URL `http://dx.doi.org/10.5194/acp-14-5295-2014`.